The Theory Behind FTIR analysis

Application Examples From Measurement at the 12 MW Circulating Fluidized Bed Boiler at Chalmers

Lars-Erik Åmand and Claes J. Tullin*

Department of Energy Conversion
Chalmers University of Technology
SE-412 96 Göteborg, Sweden

Written documentation prepared for a distance course given by The Centre of Combustion Science and Technology, CECOST on "Measurement Technology". For further details:
CECOST, Lund University
P.O Box 118, SE-221 00 Lund, Sweden
Fax +46-(0)46-222 45 42
http://www.fysik.lu.se/cecost/

* Presently at the Swedish National Testing and Research Institute, SP, Box 857, SE 501 15 Borås, Sweden, mailto:claes.tullin@sp.se, homepage: http://www.sp.se/

Introduction

FTIR Technology Applied at the Chalmers Boiler. At Chalmers University of Technology, Sweden a 12MW Circulating fluidized bed (CFB) boiler is located. At this test facility Fouirer transform infra-red (FTIR) technology has been applied for measurement of both unburned combustion gases taken from the combustion chamber as well for emission monitoring of flue gases in the stack. This paper focus on the description of the FTIR technology and evaluation procedure of FTIR spectra taken from the Chalmers boiler during coal combustion. Details of the boiler and measurement equipment are found elsewhere, Karlsson & Åmand (1996) and Karlsson et al. (1996). Data from the use of the FTIR equipment can also be found in Åmand et al. (1997), Kassman et al. (1997) and Kassman et al. 1999. The theory behind FTIR analysis given here is general but the application examples only relevant for a combustion situation like boilers, furnaces, incinerators fires and for automobile exhaust measurements. Typical for these applications are the presence of large quantities of water and carbon dioxide and sometimes hydrocarbons which makes the measurement and evaluation procedure somewhat special.

Infrared Spectroscopy. Absorption in the infrared region results in changes in vibrational and rotational status of the molecules. The absorption frequency depends on the vibrational frequency of the molecules, whereas the absorption intensity depends on how effectively the infrared photon energy can be transferred to the molecule, and this depends on the change in the dipole moment that occurs as a result of molecular vibration. As a consequence, a molecule will absorb infrared light only if the absorption causes a change in the dipole moment. Thus, all compounds except for elemental diatomic gases such as N_2, H_2 and O_2, have infrared spectra and most components present in a flue gas can be analysed by their characteristic infrared absorption.

If only one species is to be analysed, a species-specific instrument can be used. In this case analysis is carried out in a narrow wavelength interval, where the species of interest has a characteristic absorption. However, other components present in the sample may also absorb at the analytical wavelength, and for this case the spectrometer should be calibrated for cross sensitivities. For quantification of several components absorbing in the mid-infrared region (400-5000cm^{-1}), either conventional dispersive infrared analysis or Fourier Transform Infrared (FTIR) spectroscopy can be used. Compared to dispersive IR analysis, FTIR analysis is faster and has a better signal-to-noise ratio. The principles of IR analysis are discussed below.

Dispersive Infrared Spectrometers. In a double beam instrument, Fig. 1 the light from the infrared source is split into two beams. One beam passes through the sample compartment, whereas the other beam passes through the reference cell. A rotating mirror placed after the cells permits the sample and reference beams to travel in

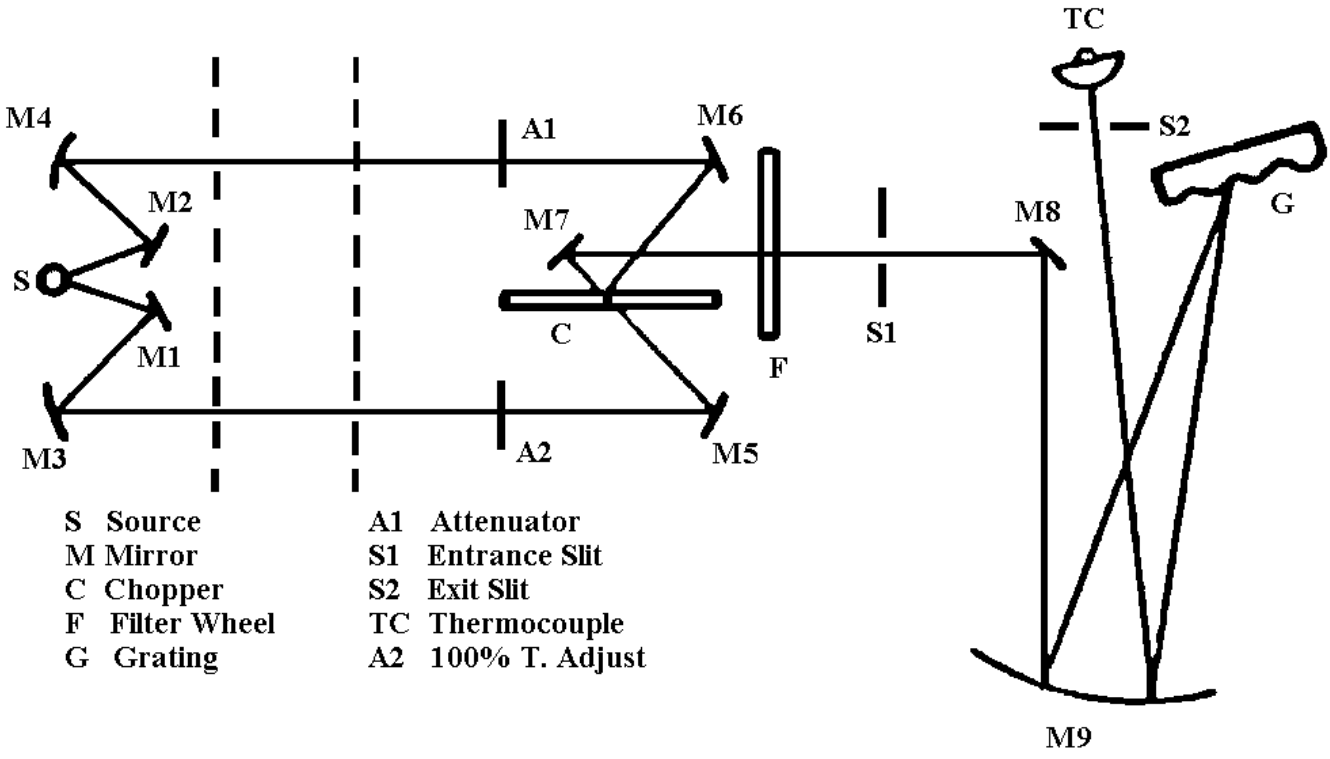

Fig. 1 Optical diagram of a dispersive infrared spectrometer..

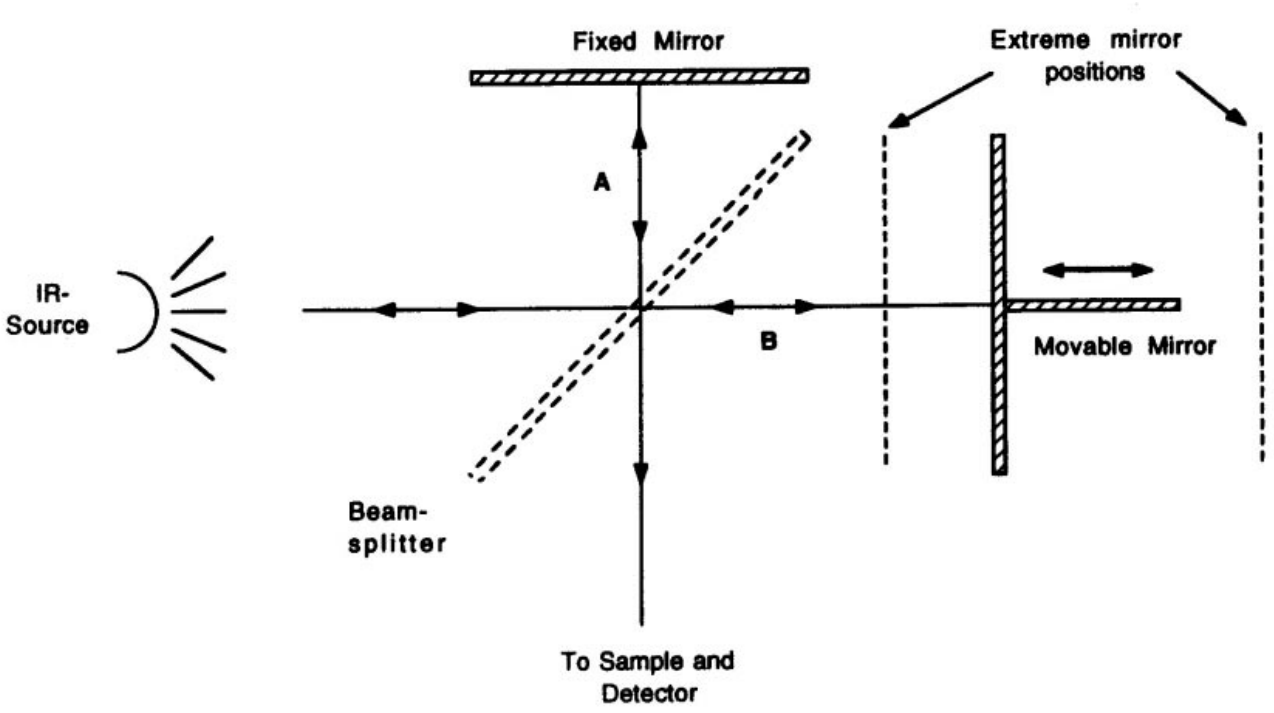

Fig. 2 Schematic diagram of the optical layout of a Michelson interferometer.

alternate pulses through the entrance slit to a monochromator (usually a grating or prism). Each pulse is dispersed, and focused onto the detector after passing the exit slit. The light energy passing through the exit slit is low resulting in a low signal-to-noise ratio. On the other hand, a larger slit would result in a lower resolution. The spectrum is produced from the difference in intensities of the sample and reference beams. In a single beam instrument, a reference (or background) spectrum and a sample plus background spectrum are collected separately. The ratio of these spectra produces the sample spectrum.

Fourier Transform Infrared Analysis (FTIR). In a FTIR instrument, the monochromator and the slits are replaced by an interferometer, usually of Michelson type. In the interferometer, a beam of radiation is divided into two beams by means of a beamsplitter. A path difference between the beams is introduced whereupon they are allowed to recombine. In this way, interference between the beams is obtained and the intensity of the output beam from the interferometer can be monitored as a function of path difference using an appropriate detector.

A sketch of an interferometer is shown in Fig. 2. Infrared radiation is projected onto the beamsplitter. An ideal beamsplitter consists of a non-absorbing film which transmits 50% of the radiation to the mirror, which is moving back and forth at a constant speed, whereas 50% of the radiation is reflected to the fixed mirror. After being reflected, the two beams will recombine at the beamsplitter where interference between the beams takes place. In order to describe how the interferometer works, let us assume that we have a monochromatic source at a wavelength λ, for example that obtained from a He-Ne laser, (λ = 632.8nm). An illustration of the output at λ = 632.8nm if passed through a suitable interferometer, would generate a cosine wave of constant frequency and intensity for the distance the mirror is moved. The result is the interferogram. This interferogram is generated by constructive and destructive interference of the light as the distance between the two arms of the interferometer is varied. This is depicted in Fig. 3A. Let y be the distance between the beamsplitter and the fixed mirror and x that between the beamsplitter and the movable mirror. The optical path difference, which is called retardation δ, between the two beams A and B is 2(y-x). If the distance between the beamsplitter and the fixed mirror is equal to that between the beamsplitter and the movable mirror (i.e y=x), the retardation is zero and the beams are perfectly in phase. As a result, the beams interfere constructively at the beamsplitter and all the light from the source will reach the detector. Displacement of the movable mirror by a distance 0.25λ will result in a retardation of 0.50λ, and the beams will be out of phase causing a destructive interference. In this case, all light returns to the source and no light reaches the detector. Thus, if one of the mirrors were moved forward, you would see light and dark bands in the output beam, corresponding to this constructive and destructive interference of the light waves, Fig. 4. Let us now consider another line source at twice the frequency or half the wavelength of our original line source from the He-Ne laser. This is depicted in Fig. 3B. Note that the wavelength of this line source is half that of pervious. This means that its frequency is double the previous. You will note that the amplitude of the cosine wave is equivalent to the intensity of the line source, while the frequency of the cosine wave relates to the frequency or wavelenght of the line source. The third example is to consider the result of placing the two line sources through the interferometer

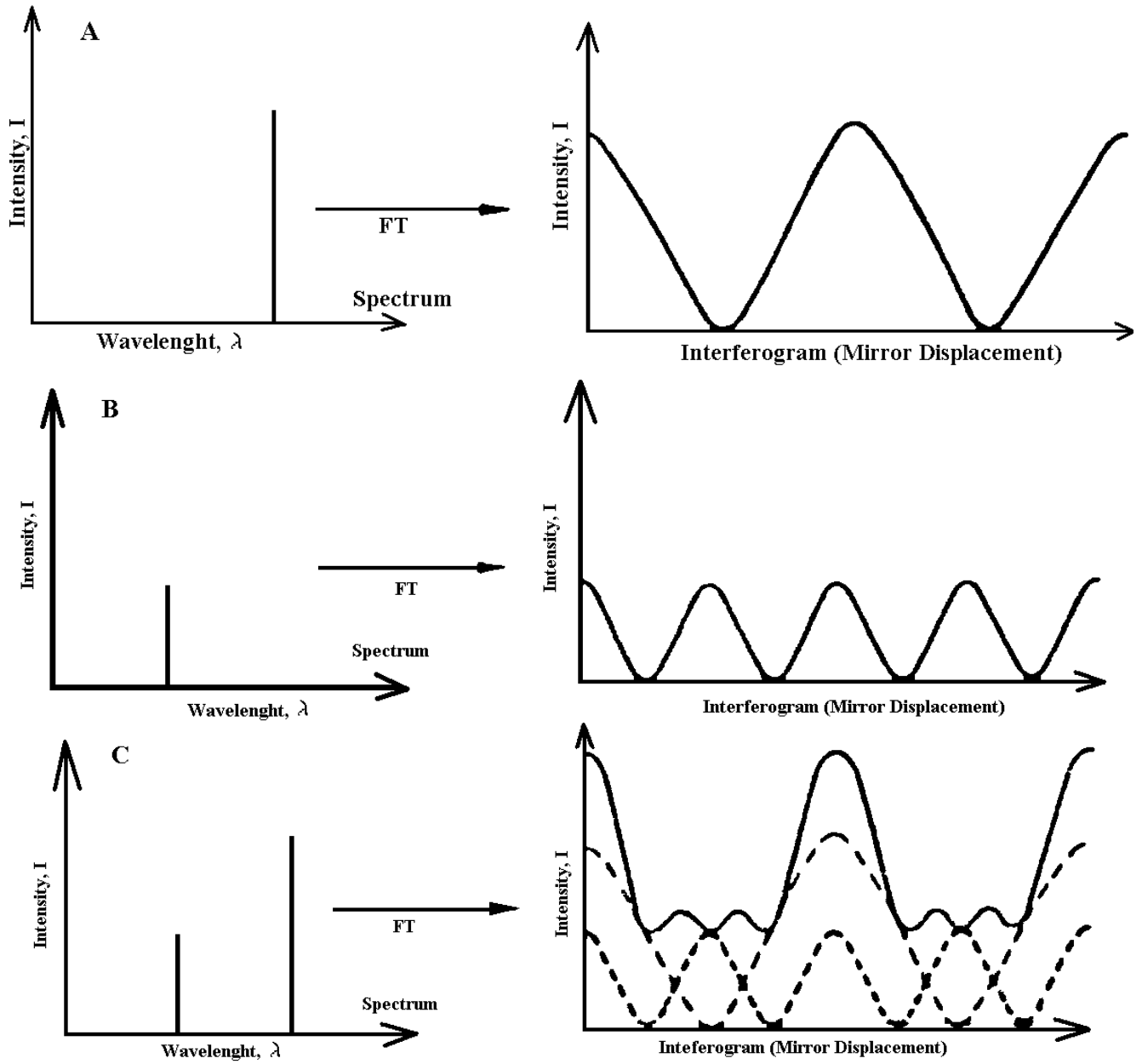

Fig. 3 A He-Ne laser line passed through interferometer.
B Laser line 0.5 intensity and 0.5 λ of He-Ne passed through interferometer.
C Both line sources passed through interferometer.

simultaneously. Each would generate is own interferogram, Fig. 3C. In the instrument, these will be measured together and the end result will be the sum of two individual line sources. Mathematically the signal treatment can be described in the following way: If I(x) is the intensity of the beam measured at the detector at a diplacement of the movable mirror by x cm, and if B(ν) represents the intensity of the source as a function of frequency ν , the equation for the signal at the detector (i.e. the interferogram) can be written:

$$I(x) = B(\nu)\cos 2\pi\nu x$$

For a dichromatic source (with frequencies ν_1 and ν_2), the signal at the detector is the sum of two cosine waves:

$$I(x) = B(\nu_1)\cos 2\pi\nu_1 x + B(\nu)\cos 2\pi\nu_2 x$$

For a polychromatic source, as in a real instrument, the detector signal, the interferogram is related to the spectrum by:

$$I(x) = \frac{1}{2\pi}\int_{-\infty}^{+\infty} B(\nu)\cos 2\pi\nu x d\nu \qquad (1)$$

The spectrum is related to the interferogram by the following:

$$B(\nu) = \int_{-\infty}^{+\infty} I(x)\cos 2\pi\nu x dx \qquad (2)$$

Eq. 1 and 2 relates an interferogram to an infrared single-beam spectrum via the mathematics of the Fouier transform. The signal described by eq. 1 is more or less

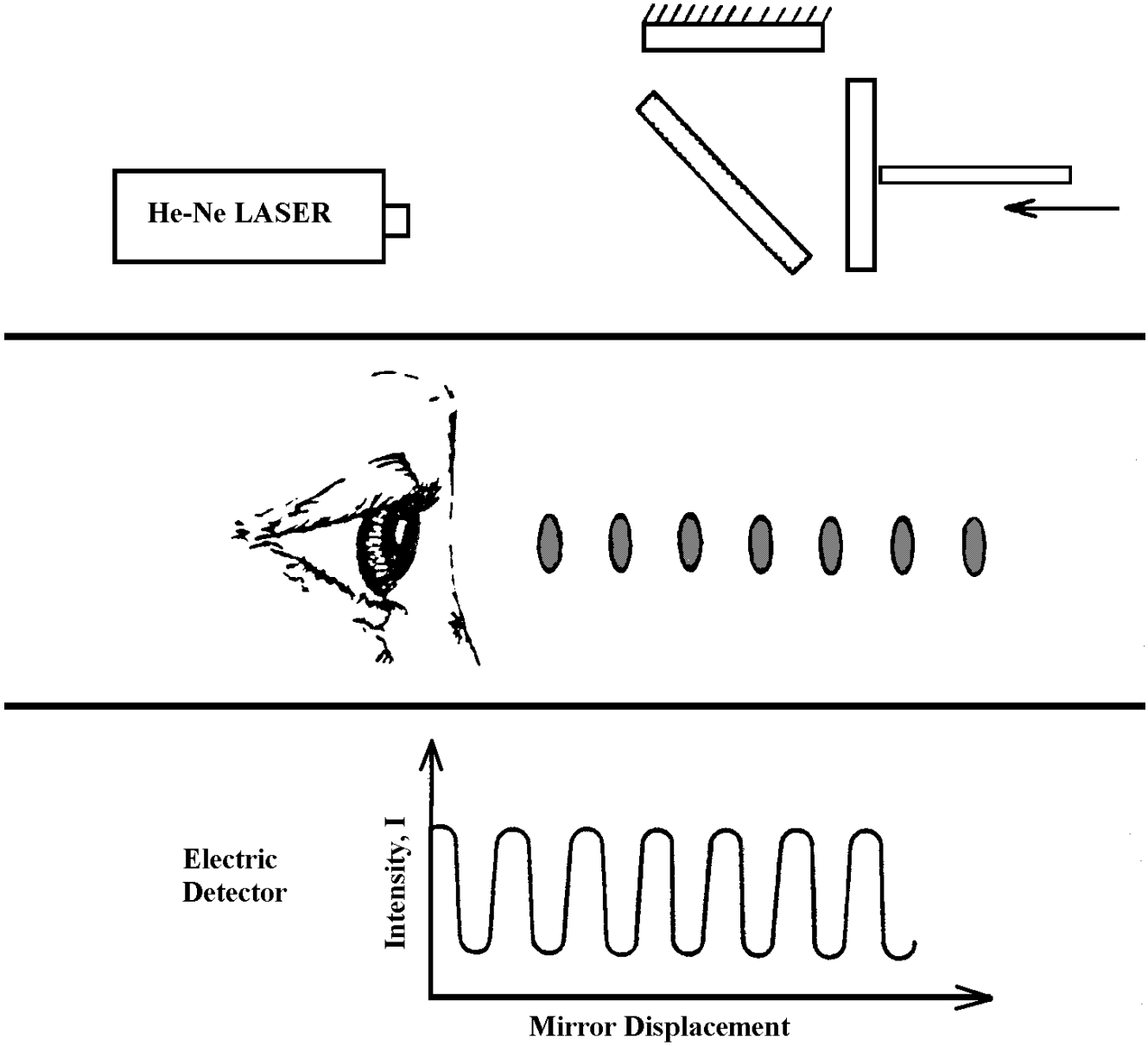

Fig. 4 He-Ne laser line passed through interferometer.

constant during the mirror scan, but when the mirrors are equidistant from the beamsplitter all waves are in phase and the interferogram shows a so called centre burst. An example of a real interferogram, i.e a plot of the intensity measured at the detector as a function of retardation, is shown in Fig. 5. Assume that we have sampled an interferogram for the reference case, i.e. when the gas cell is filled with reference gas. The interferogram so obtained is described by eq.1, whereas the corresponding single beam spectrum is described by eq. 2. Let us assume that we fill the cell with a sample containing a species which absorbs light at one frequency. The interferogram obtained then is the reference interferogram with a cosine wave corresponding to the frequencies of the absorbing species subtracted. In the real case, absorption occurs at many frequencies and the sample interferogram is composed of all frequencies except those absorbed by the sample.

Since the movable mirror travels a finite distance from -x to +x, the interferogram cannot extend from -infinity to +infinity (cf. Eq. 1), and it is in practise truncated. The truncation function that is unity between -x and +x and zero at all other points is called the boxcar truncation function. The Fourier transformation of a truncated interferogram results in a spectrum where the peaks have side lobes. Suppression of these side lobes is known as apodization and can be obtained by multiplying the interferogram with a suitable weighting function such as the triangular function instead of using the boxcar function The results reported here were, however, obtained using the boxcar truncation function.

Qualitative Analysis

As pointed out for example by Smith (1979), the infrared absorption spectrum of a compound is highly individual, or in his words: "In most instances the IR spectrum is a unique molecular fingerprint that is easily distinguished from the absorption patterns of other molecules. " Since most of the components in a flue gas are IR active it should be possible to characterise the composition of the

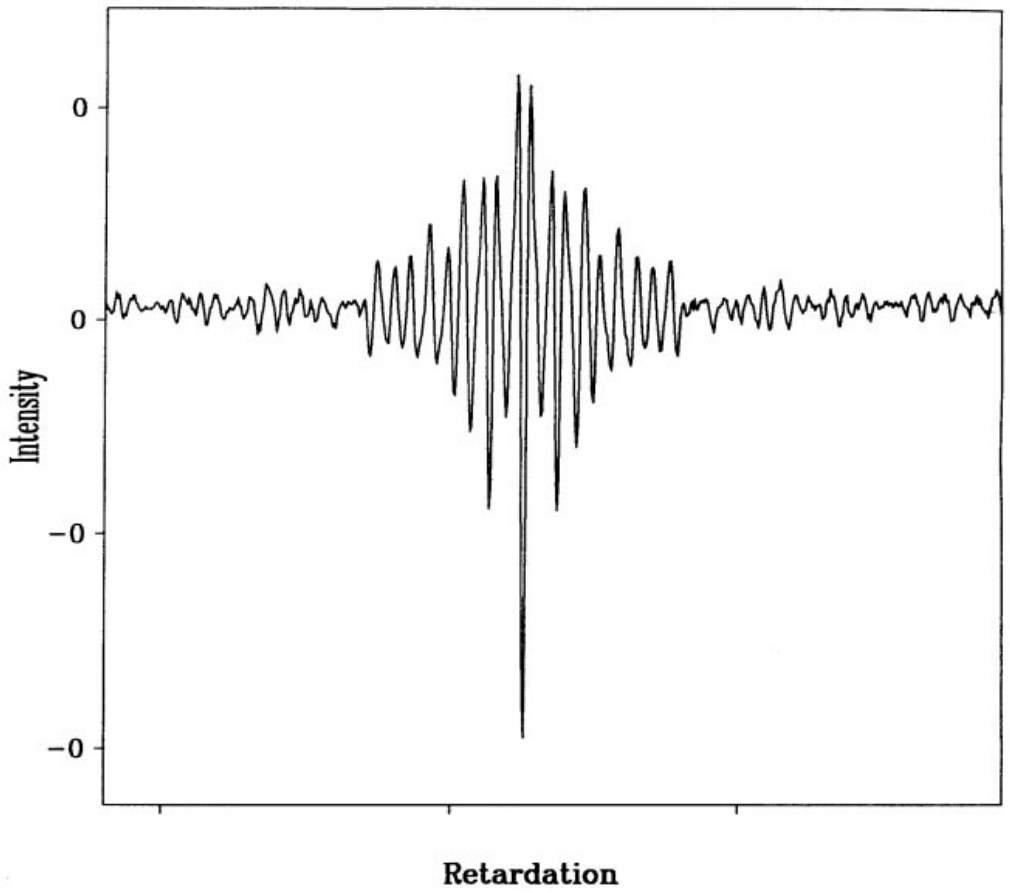

Fig. 5 Interferogram, i.e a plot of the intensity measured at the detector as a function of retardation

gas. However, in combustion gases a major problem is the presence of water vapour and carbon dioxide which absorb in broad bands in the IR spectrum. In addition, their high concentration result in a high absorption compared to trace components of interest. Griffiths and de Haseth (1986) pointed out that subtracting two peaks of high absorption, such as subtracting CO_2 from a flue gas spectrum, can result in a residual absorbance peak caused by deviations from Beer´s law rather than by the presence of an additional absorbing species. Nevertheless, as will be shown below it is possible to detect trace components where carbon dioxide and water vapour interfere.

Quantitative Analysis

For a beam of parallel monochromatic light of intensity I_0 through a homogeneous and infinitesimally thin layer, Bouguer found that the decrease in intensity is proportional to the layer thickness and the intensity of the radiation. The same law relating the absorption of a material to its thickness was later independently stated by Lambert. Beer showed that for a given layer thickness (l), the transmittance $\tau(\nu)$ (i.e. the ratio of the transmitted and incident radiation) decreases proportionally with increasing concentration (c). For a single component the Bouguer-Lambert-Beer law) can be written,

$$A(\nu) = -\log_{10} \tau(\nu) = -\log_{10} I/I_0 = a(\nu)lc \qquad (3)$$

Where $A(\nu)$ is the absorbance and $a(\nu)$ the absorptivity. For a multicomponent mixture eq.3 becomes,

$$A(\nu) = \sum_{i=1}^{N} a_i(\nu) l c_i \qquad (4)$$

In most cases a plot of absorbance versus concentration shows a non-linear dependence. Deviations from Beer´s law can be a result of stray radiation, chemical effects and -most important- insufficient resolution (Griffiths and de Haseth, 1986). The effect of resolution on true and apparent absorbance has also been discussed by Brink, 1992. Beer´s law is strictly valid only for monochromatic radiation and if the resolution is too low this will result in a non-linear behaviour.

Spectral Subtraction. The amount of a substance present in a sample can be determined by computerised spectral subtraction. Single beam spectra can be collected for the sample and for a calibration gas (containing the species of interest at an appropriate concentration). These spectra are rationed against a background spectrum (such as one obtained with the cell filled with nitrogen) to produce an absorbance spectrum (cf. eq. 3). In order to determine the

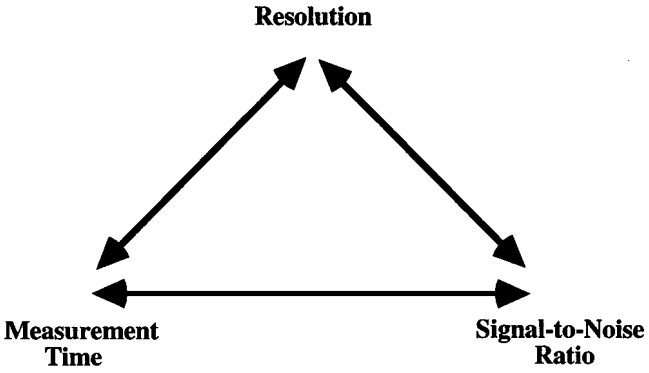

Fig. 6 Trade-off between resolution, signal-to-noise ratio (SNR) and the time required to perform the measurement.

absorbance of a species, the corresponding calibration spectrum is then subtracted from the sample spectrum. Generally, the species concentration in the sample is different from that of the reference, and the calibration spectrum is multiplied by a suitable factor (F) in such a way that:

$$A_{sample}\text{-}F \times A_{cal.spectrum} = 0 \qquad (5)$$

If absorbance *vs* concentration plot is linear, the concentration of the species is simply the concentration in the reference times the factor F. However, deviations from Beer´s law at higher absorption can be expected and Griffiths and de Haseth (1986) give as a rule of thumb for absorbance units of 0.7 or higher, accurate subtraction can only be obtained using references of a concentration very close to that of the sample (F≈ 1 in eq. 5). However, for broad bands (i.e with a resolution parameter $\rho \leq 0.1$) it is possible to obtain linear plots of absorbance *vs* concentration for absorbancies up to 2 absorbance units (Griffiths and de Haseth, (1986). The resolution parameter is defined as:

$$\sigma = \frac{\text{instrumental resolution}}{FWHH} = \frac{1}{\Delta_{max} \times FWHH} \qquad (6)$$

where Δ_{max} is the maximum retardation of the interferometer and FWHH is the full with of the peak at half-height.

It should be noted that there is a trade-off between resolution, signal-to-noise ratio (SNR) and measurement time as illustrated in Fig. 6. At a given resolution the SNR is proportional to the square root of the measurement time, i.e to the number of scans. It may therefore prove worthwhile to increase the number of scans collected to produce a spectrum if peaks of weak absorbanced are to be used for analyses. On the other hand, if the measurement time, optical throughput and the velocity of the moving mirror are constant, a sample spectrum collected at a higher resolution will have a lower SNR than a spectrum collected at a lower resolution. However, the resolution may also affect the peak absorptance, i.e. the percentage of the incident being absorbed at the band center ($[1-\tau(\nu)]x100\%$). For a week spectral feature, the absorptance of a narrow peak with the FWHH much less than the instrumental resolution will approximately double on increasing the resolution with a factor of two. Thus, the optimum SNR is obtained when the measurements are performed at the lowest spectral resolution that adequately resolves the peaks of interest from overlapping lines. At a given resolution the SNR is proportional to the square root of the measurement time, i.e to the number of scans, and for weak absorbances it may be advantageous to increase the number of scans.

Examples of subtractions are given below where the procedures for the HCN, HNCO and NH_3 analyses are discussed. The spectra were collected using a Bomem M100-D11 with a 500cm^3 quartz glass gas cell with an optical path length of 3.6 m. The instrument was equipped with a MCT detector and the resolution was 4 cm^{-1}. The

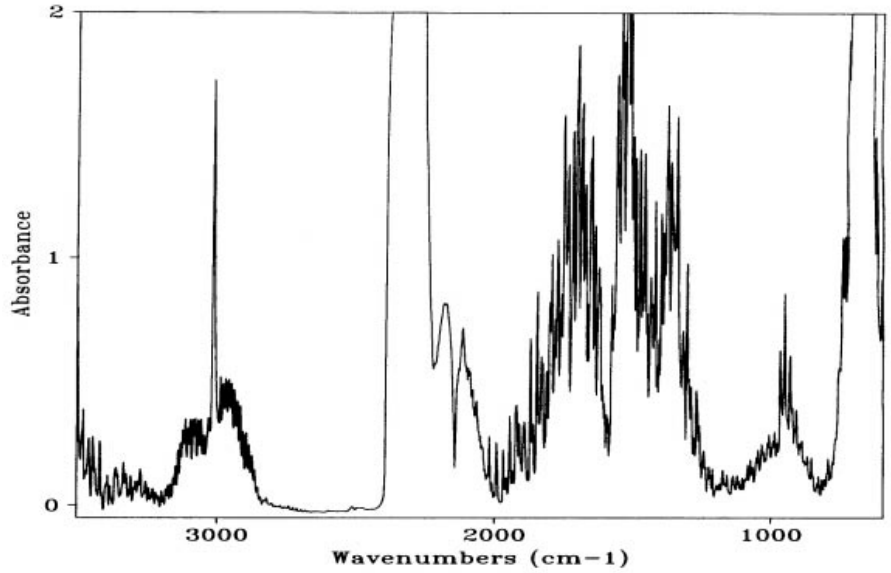

Fig. 7 A typical spectrum of a gas sample of combustion gas taken from the combustion chamber.

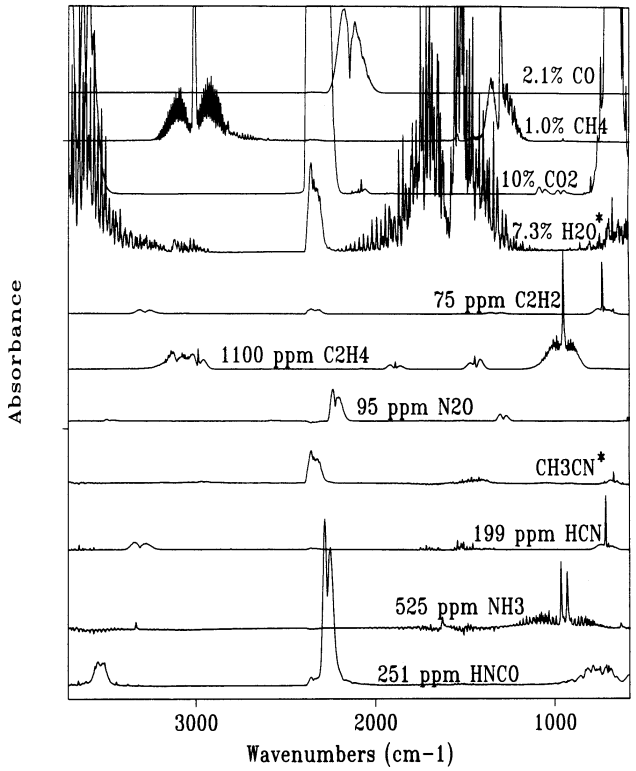

Fig. 8 Spectra for some major and minor flue gas components (all spectra are shown at the same scale in order to enable comparison of absorbances). *) The peaks at 600-750 cm^{-1} and 2200-2400 cm^{-1} are due to the presence of small amounts of CO_2.

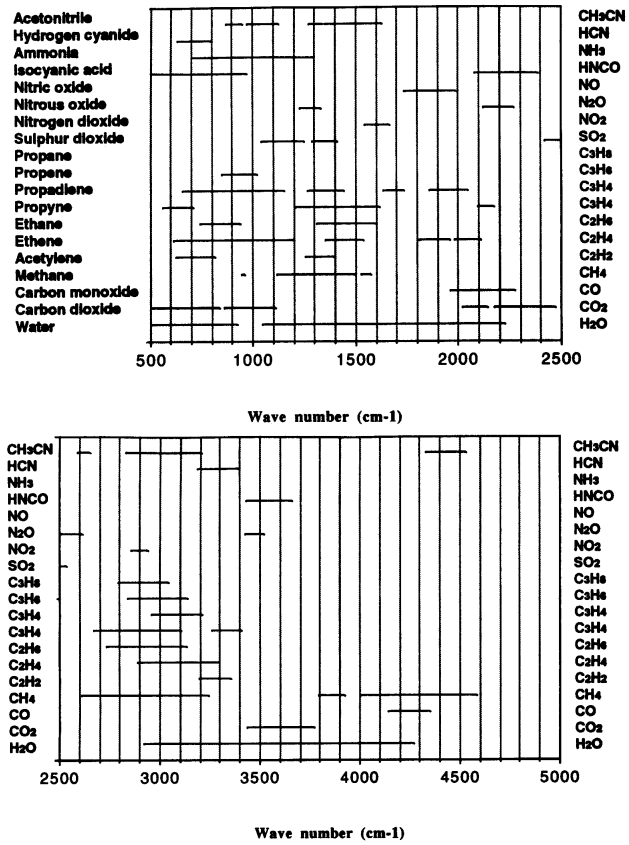

Fig. 9 Absorption bands between 500-2500cm^{-1} (upper) and 2500-5000 cm^{-1} (lower) for some species present in combustion gases.

gas cell as well as the tubing was heated to 175 °C. The Spectra Calc software package was used for evaluation and control of the spectrometer. About 10 to 15 single beam spectra (22 scan each) were co-added to form an "average" single beam spectrum. An absorbance spectrum was then produced from the ratio of the average single beam spectrum and a reference spectrum (100% nitrogen) collected immediately before the sample spectrum.

Results

In Fig. 7, a typical spectrum of a gas sample of combustion gas taken from the combustion chamber is shown. The reference spectra for the major components CO_2 and H_2O as well as for trace components such as NH_3, HCN and HNCO are shown in Fig. 8. A larger number of components present in combustion gases and their respective bands of absorption are shown in Fig. 9. In an ideal case it is possible to find an isolated wave number band where only the substance of interest absorbs. It is clear from the figures that there are no such regions for any of the trace components mentioned. In addition, quantitative analyses of multiple component mixtures can be complicated by interferences (matrix effects) in such a way that the spectrum for the mixtures differs from the spectrum obtained if the spectra for all pure components were co-added. Rudling (1992) discusses FTIR analysis of CO_2, H_2O, CO, N_2O, NO, NO_2, SO_2 and NH_3 and report matrix effects for mixtures of CO_2 and H_2O and for the system N_2O-CO_2 system at ca 2200 cm^{-1}. In the analyses

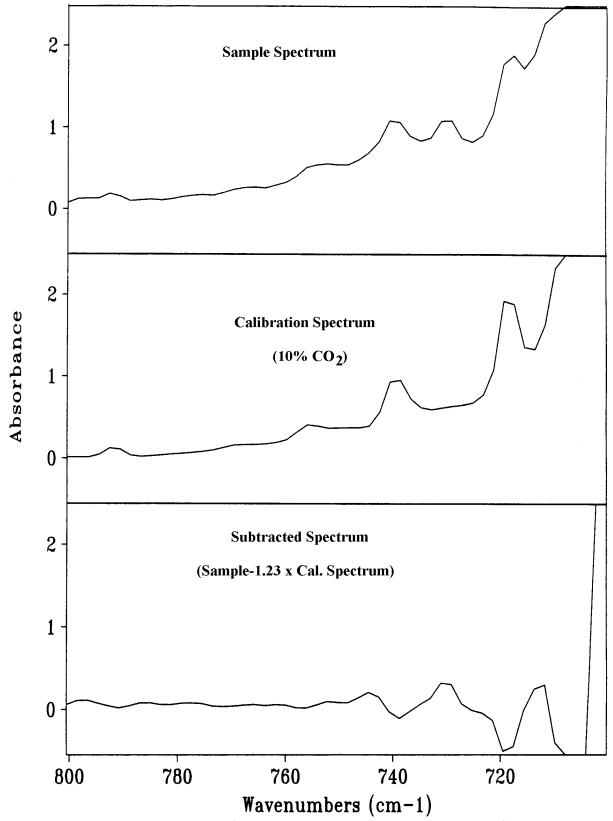

Fig. 10A Subtraction of CO_2 calibration spectrum from a sample spectrum at ca 700-800 cm^{-1}.

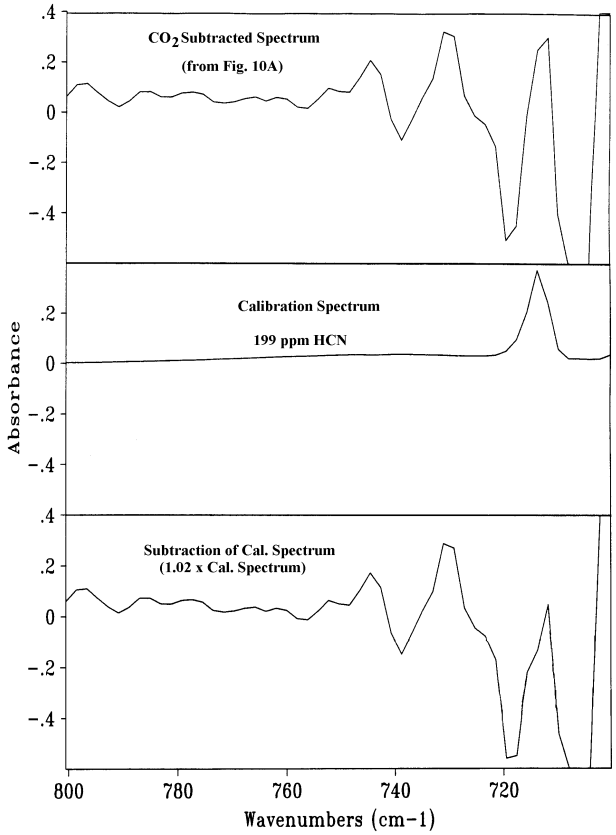

Fig. 10B Subtraction of a HCN calibration spectrum from a sample spectrum at ca 700-800 cm^{-1}.

reported below, matrix effects were assumed to be negligible.

HCN Analysis. From the reference spectra in Fig. 8 it can be seen that HCN absorbs in two regions. Its strongest peak at 714 cm^{-1} interferes mainly with the CO_2 absorption. The subtraction of a calibration spectrum of CO_2 from a sample spectrum cf. Eq. 5) is shown in Fig. 10a, and the subsequent subtraction of a HCN calibration spectrum is shown in Fig. 10b. The "HCN peak" that appears at ca 714 cm^{-1} after the CO_2 subtraction (see Fig. 10b) may be a result of the subtraction. As discussed above, caution is needed when the absorbance is higher than 0.7 and since the resolution parameter is too high (with the present instrument $\rho \approx 4cm^{-1}/4cm^{-1}=1.0$, cf. eq. 6) it is not possible to say whether the apparent absorption at 714 cm-1 is due to the presence of HCN in the sample, or if it is an effect of an inadequate subtraction. A higher spectral resolution would be required to use this band for HCN quantification of the flue gases. Alternatively, the total absorption of the sample can be reduced to acceptable values simply by diluting the sample with a non-absorbing gas such as N_2 prior to the FTIR analysis. To reduce the maximum absorbance to 0.5 with the present instrument, the sample should be diluted to 1.5-2.5% CO2. Consequently, if the HCN concentration is high enough, dilution would enable a successful quantification at 714 cm^{-1}.

Although the absorption is weaker, an alternative band for HCN quantification is located at 3200-3375 cm^{-1}. In

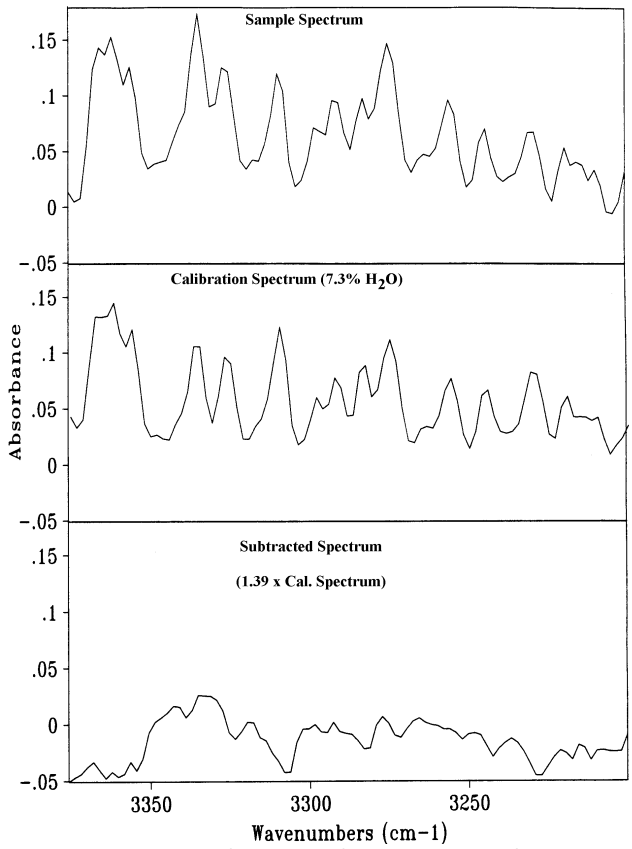

Fig. 11A Subtraction of a water reference spectrum from a sample spectrum at 3200-3375 cm^{-1} (Sample position H3CC, cf. Table 1).

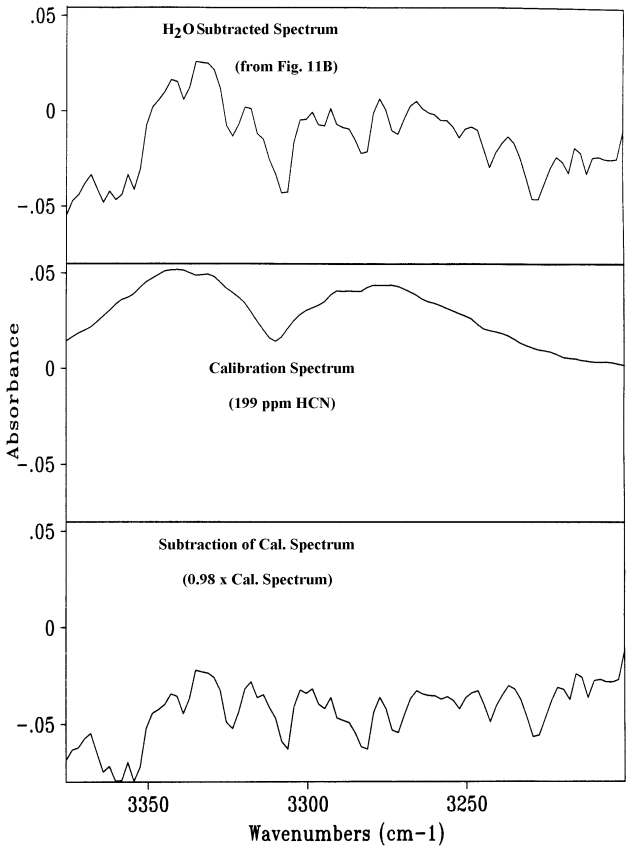

Fig. 11B Subtraction of a HCN calibration spectrum from a sample spectrum at 3200-3375 cm^{-1}.

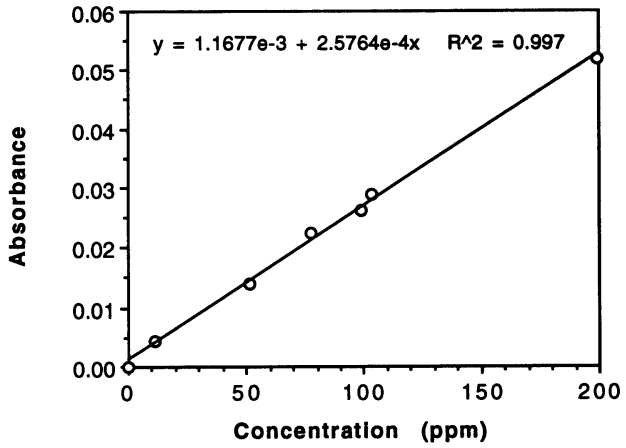

Fig. 12 Absorbance *vs*. concentration for HCN at 3343cm^{-1}.

this region water has to be subtracted from the sample spectrum prior to HCN (see Fig. 11A). After the water subtraction, the double peak of HCN clearly appears on the spectrum which can be seen in Fig. 11B, where the subsequent subtraction of HCN is shown. The absorbance in this region is low (as the resolution parameter, since the subtraction is performed for a broad band) and Beer´s law can be expected to be obeyed. Indeed, this is the case as seen in Fig 12 where the peak absorbance at 3343 cm^{-1} for the HCN standards is plotted as a function of concentration.

Consequently, the HCN concentrations in the sample spectra obtained from the measurements in the Chalmers Boiler were quantified using the band at 3200-3375 cm^{-1}. Since the absorbance is low enough for Beer´s law to be valid, all subtractions were performed using the same H2O and HCN standards (i.e. the water reference corresponding to satuartion at atmospheric pressure at 40°C (7.3% H_2O)

Table 1. Subtraction factors obtained for the estimation of HCN concentrations.

Sampling position	Height above nozzles (m)	Subtraction factors		
		H_2O (40°C)[1]	199 ppm HCN	
			"Best"	Min./Max.
H2CC	0.65	1.59	1.2	1.0/1.4
H3CC	1.1	1.39	0.98	0.85/1.15
H4BC	1.6	1.16	0.95	0.85/1.05
H4CC	1.6	1.125	0.80	0.70/0.90
H4FC	1.6	1.37	0.59	0.5/0.7
H45CC	2.0	1.24	0.70	0.65/0.75
H8BC	4.3	0.83	0.0	-0.15/0.15
H8CC	4.3	1.25	0.25	0.1/0.4
H8FC	4.3	1.43	0.15	0.0/0.3
H9CC	4.8	1.31	0.15	0.0/0.3
H10CC	5.95	1.29	0.15	0.0/0.3
H11CC	8.0	1.25	0.05	-0.1/0.2
H12CC	10.0	1.30	0.00	-0.1/0.1
H13CC	11.0	1.25	0.0	-0.1/0.1

[1]Reference prepared by saturating a stream of N_2 with water at 40 °C at atmospheric pressure (corresponds to ca 7.3% H_2O).

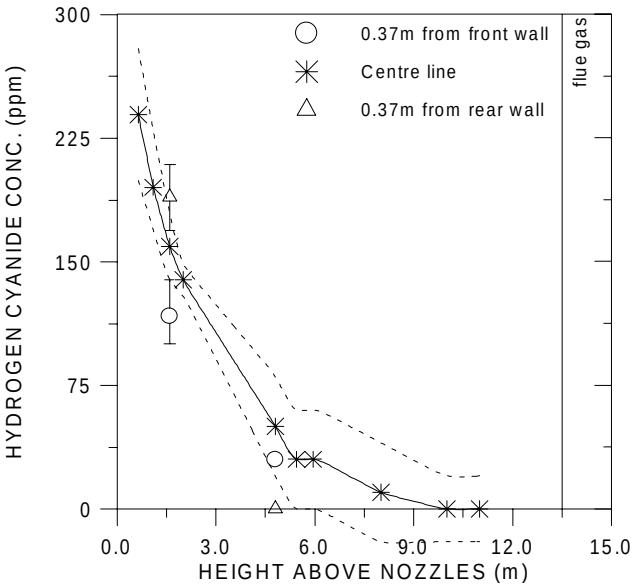

Fig. 13 Vertical profiles of HCN in the combustion chamber. Dotted lines indicate the uncertainty in the HCN determination.

and 199 ppm HCN). The main difficulty performing the subtraction in this special region is that the signal-to noise-ratio is low. The spectral subtractions were carried out manually, and the subtraction factors were estimated by visual observation. In order to estimate the accuracy of the analyses, both minimum and maximum values of the subtractions factors were estimated, as well as a "best" value. Although the low SNR makes absolute concentration predictions difficult, the analysis gives an indication of the magnitude of the HCN concentrations. In relative terms the obtained values can be compared. The subtraction factors are listed in Table 1 and the HCN

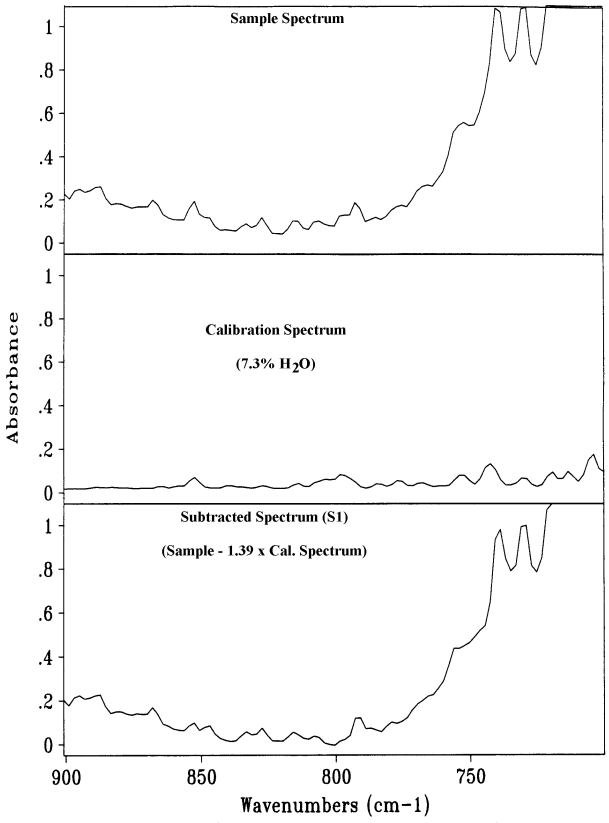

Fig 14A Subtraction of water calibration spectrum from a sample spectrum at 700-900cm^{-1} (sample position H3CC, cf. Table 2).

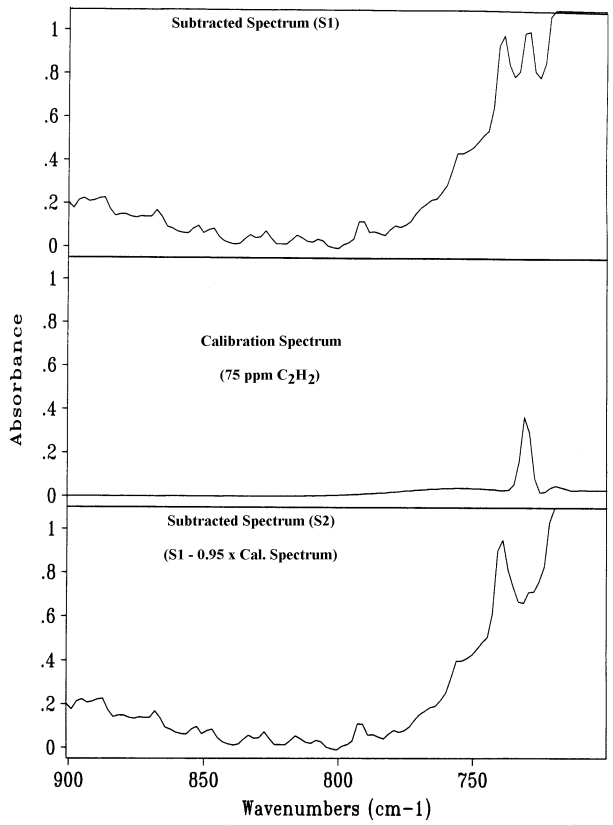

Fig. 14B Subtraction of an acetylene calibration spectrum from a sample spectrum at 700-900cm^{-1}.

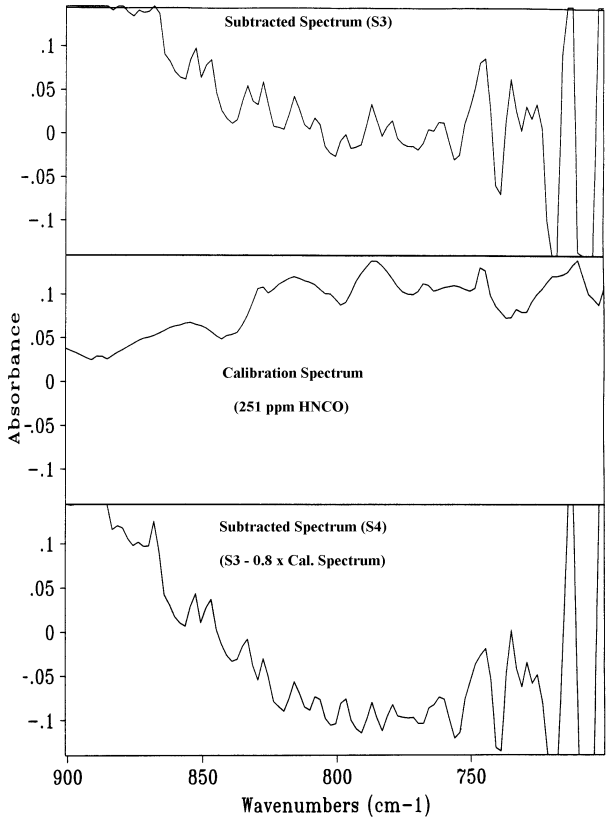

Fig. 14D. Subtraction of a HNCO calibration spectrum from a sample spectrum at 700-900cm^{-1}.

concentrations were calculated assuming that Beer´s law was valid (cf. Fig. 12). The resulting concentrations are reported in Table 4 and the HCN profile is shown in Fig. 13. The minor interference with the HCN absorption caused by the presence of ethene and acetylene was not considered. In addition, CH_3CN, propadiene and propyne would interfere in this region but the concentrations of these species were found to be below detection limit.

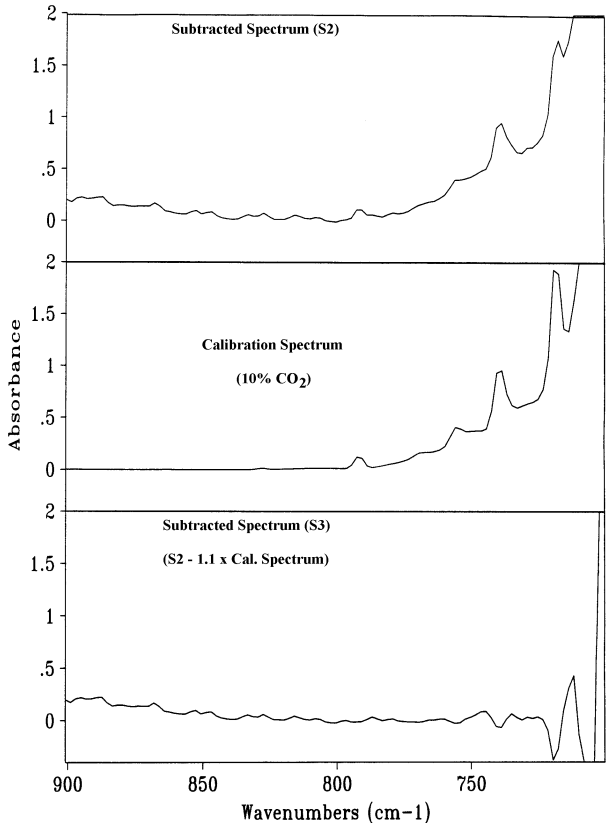

Fig. 14C Subtraction of a CO2 calibration spectrum from a sample spectrum at 700-900 cm^{-1}.

HNCO Analysis. HNCO absorbs in three regions in the infrared, Fig. 8) The high concentration of CO_2 in the flue gas makes it impossible to perform the subtraction at the main HNCO peak at 2280 cm^{-1}, as well as at the second strongest peak at ca 3500 cm^{-1}, with the present instrument due to too low resolution (as for HCN, dilution of the sample prior to FTIR analysis may provide the necessary tool for a successful quantification of HNCO where it interferes with CO_2). However, it is possible to perform the subtraction for the absorption peak below 1000 cm^{-1}. In this region, the HNCO absorption interferes with a large number of components. The HNCO concentration was estimated after subtraction of water, and carbon dioxide at 700-900 cm^{-1} Fig 14a-d). Since it is difficult to determine the subtraction factor for water in this region, the factor estimated at 3200-3375 cm^{-1} was used. The same reference spectra (7.3 % H_2O, 75 ppm C_2H_2, 10% CO_2 and 251 ppm HNCO) were used for all determinations. In Fig. 15, the plot of peak absorbance at 787 cm-1 *vs.* concentration for the HNCO standards is shown to display a linear dependence. The shape of the absorbance spectrum obtained after subtractions of the interfering components (i.e. after the subtraction of water, acetylene and carbon dioxide) indicates the presence of HNCO which appears as a double peak with a minimum at ca 800 cm-1 (cf. Fig.

Table 2 Subtraction factors obtained for the estimation of HNCO concentrations.

Sampling position	Height above nozzles (m)	Subtraction factors				
		H_2O (40°C)[1]	75 ppm C_2H_2	10% CO_2	251 ppm HNCO	
					"Best"	Min./Max.
H2CC	0.65	1.59	0.98	1.125	1.0	0.0/2.0
H3CC	1.1	1.39	0.95	1.07	0.8	0.4/0.95
H4BC	1.6	1.16	0.73	1.05	0.4	0.1/0.7
H4CC	1.6	1.125	0.68	1.0	0.34	0.1/0.5
H4FC	1.6	1.37	1.20	1.05	0.60	0.3/0.9
H45CC	2.0	1.24	0.95	1.06	0.41	0.2/0.6
H8BC	4.3	0.83	0.13	0.84	0.15	0.0/0.3
H8CC	4.3	1.25	0.63	1.06	0.2	0.1/0.3
H8FC	4.3	1.43	0.44	0.77	0.25	0.0/0.5
H9CC	4.8	1.31	0.55	1.1	0.3	0.1/0.6
H10CC	5.95	1.29	0.58	1.03	0.3	0.2/0.4
H11CC	8.0	1.25	0.28	1.04	0.2	0.0/0.4
H12CC	10.0	1.3	0.23	1.01	0.3	0.0/0.4
H13CC	11.0	1.25	0.2	0.89	0.1	-0.1/0.3

[1]Reference prepared by saturating a stream of N_2 with water at 40 °C at atmospheric pressure (corresponds to ca 7.3% H_2O).

14d). It should be noted that the result is merely an indication of the presence of HNCO in the sample rather than absolute proof. The subtraction factors and the corresponding concentrations are reported in Table 2 and 4, respectively. The HNCO concentrations *vs.* bed height is shown in Fig. 16. It should be noted that also HCN, NH_3, CH_3CN, ethene, ethane and propadiene absorb at 700-900 cm^{-1}. Subtraction of reference spectra for these species (CH_3CN, ethane and propadiene were not detected) in addition to water, acetylene and carbon dioxide results in slightly lower subtraction factors.

NH_3 Analysis. Ammonia has two distinct absorption peaks at 930 cm^{-1} and 965 cm^{-1}, respectively (Fig. 8). The major interfering components at this frequency are ethene

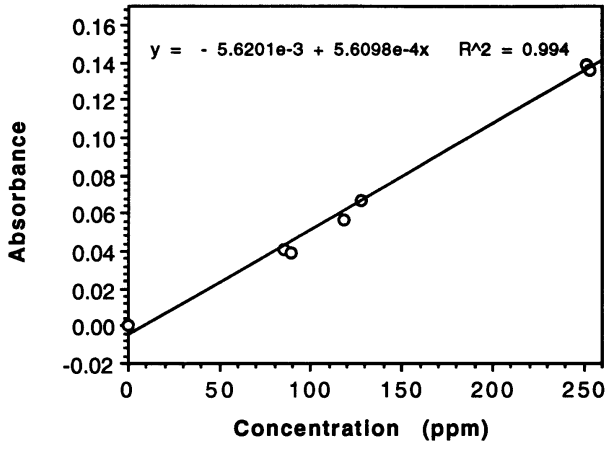

Fig. 15 Absorbance vs. concentration for HNCO at 787cm^{-1}.

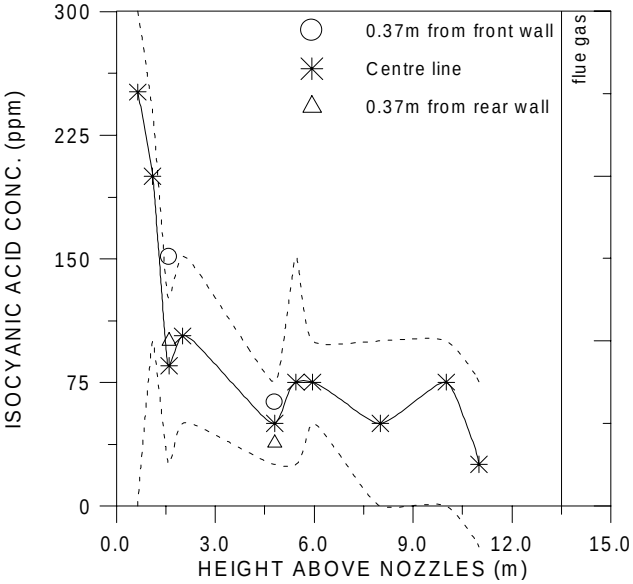

Fig. 16 Vertical profiles of HNCO in the combustion chamber. Dotted lines indicate the uncertainty in the HNCO determination

and HNCO, whereas carbon dioxide, and for the peak at 930 cm^{-1} also propene, propadiene and acetonitrile, absorb weakly (Fig. 8). Propadiene and acetonitrile were not detectable using the present instrument. The spectra resulting from the HNCO estimation (see previous section) were used as a starting point for the NH_3 quantification.

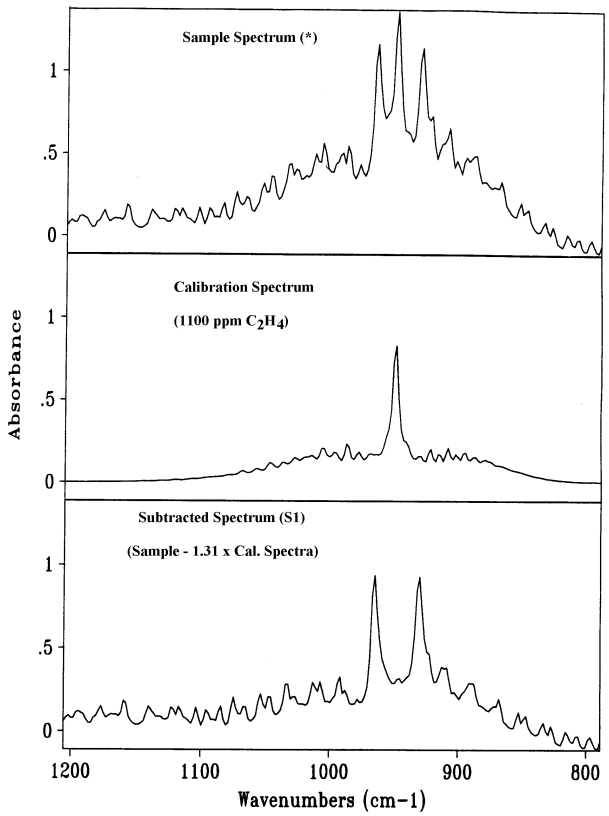

Fig. 17A Subtraction of ethene calibration spectrum from a sample spectrum at 800-1200cm-1 (sample position H2CC, cf. Table 3). (*) The sample spectrum is that obtained in the HNCO quantification corresponding to S4 in Fig. 14D.

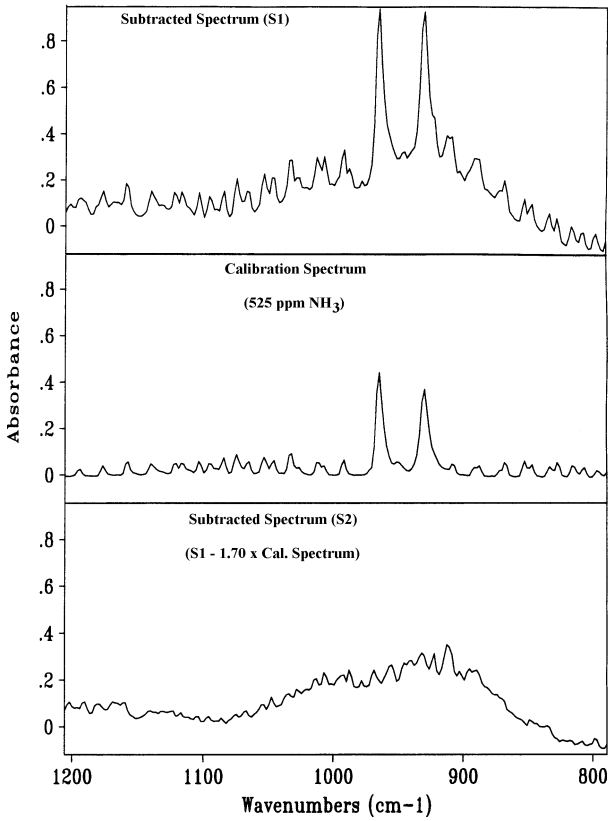

Fig. 17B Subtraction of an ammonia calibration spectrum from a sample spectrum at 800-1200cm^{-1}. The peak at 965cm^{-1} was minimised.

Table 3. Subtraction factors obtained for the estimation of NH_3 concentrations.

Sampling position	Height above nozzles (m)	Subtraction factors		
		1100 ppm Ethene	525 ppm NH_3	
			"Best"	Min./Max.
H2CC	0.65	1.31	1.83[1)]	
H2CC	0.65		1.70[2)]	1.50/1.90
H3CC	1.1	0.93	0.99[3)]	0.89/1.09
H4BC	1.6	0.42	0.39	0.33/0.42
H4CC	1.6	0.52	0.29	0.25/0.32
H4FC	1.6	0.79	0.34	0.24/0.37
H45CC	2.0	0.57	0.37	0.29/0.39
H8BC	4.3	0.018	0.0	-0.01/0.01
H8CC	4.3	0.18	0.01	-0.001/0.02
H8FC	4.3	0.07	0.0	-0.01/0.01
H9CC	4.8	0.12	0.01	-0.01/0.02
H10CC	5.95	0.13	0.01	-0.01/0.02
H11CC	8.0	0.03	0.006	-0.002/0.014
H12CC	10.0	0.02	0.006	-0.002/0.014
H13CC	11.0	0.01	0.01	0.002/0.01

1) Subtracted minimising the peak at 930 cm^{-1}.

2) Subtracted minimising the peak at 965 cm^{-1}.

3) At this sample position and above, no differences between the absorption at 930 cm^{-1} and 965 cm^{-1} were obtained.

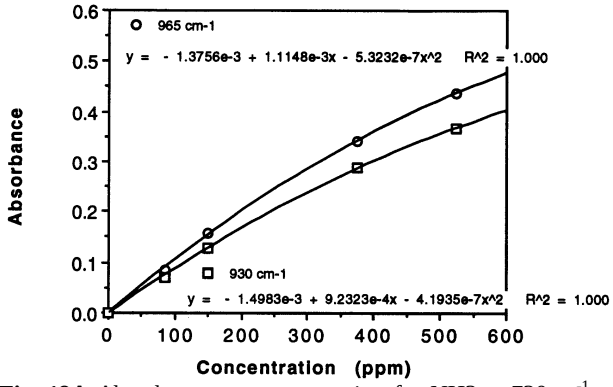

Fig. 18A Absorbance *vs.* concentration for NH3 at 730cm^{-1} and 765cm^{-1}. Second order polynomial fit.

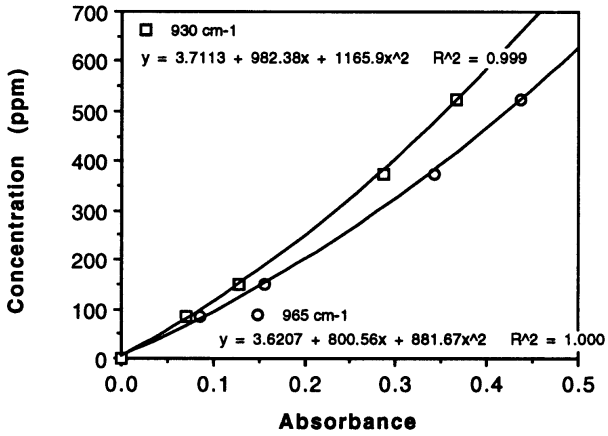

Fig. 18B Calibration plot used in the quantification of NH_3.

Thus, HNCO and carbon dioxide were subtracted from the spectra with factors given in Table 2. The subtraction of water and acetylene which was carried out in the HNCO estimation, does not affect the ammonia peaks since these components do not absorb at this frequency. The subtraction of ethene from a spectrum of a measurement in the lower part of the combustion chamber (0.65 m above the nozzles) in the Chalmers CFB boiler is shown in Fig. 17a. The subsequent subtraction of ammonia is shown in Fig. 17b. At this position, a slightly higher value was obtained when the subtraction was performed for the peak at 930 cm^{-1} compared to when the peak at 965 cm^{-1} was minimised cf. Table 3). The difference is not significant although it can be noted that some combustion gas components such as propene have a higher absorption at 930 cm^{-1} than at 965 cm^{-1}. Subtraction of propene from the sample spectrum did not influence the quantification of NH_3 significantly, and at all other sample positions higher up in the combustion chamber, where the hydrocarbon concentration is lower, the subtractions yield approximately the same number at both frequencies. The peak absorbance versus concentration for NH_3 can be fitted by a second order polynome (Fig. 18a). In all subtractions a calibration spectrum of 525 ppm NH_3 was used. The subtraction factors obtained are listed in Table 3. The absorbance corresponding to subtraction of the calibration spectrum F x $A_{cal.spectrum}$ in eq. 5) was used to estimate the concentration from the concentration *vs.*

Table 4. Concentrations of HCN, HNCO and NH_3 *vs* sampling positions from data given in Tables 1-3.

Sampling position	Height above nozzles (m)	HCN best (ppm)	HCN min/max (ppm)	HNCO best (ppm)	HNCO min/max (ppm)	NH_3 best (ppm)[1]	NH3- min/max (ppm)[1]
H2CC	0.65	239	279/299	251	0/502	1086	908/1277
H3CC	1.1	195	169/229	201	100/238	515	449/585
H4BC	1.6	189	169/209	100	25/176	166	137/180
H4CC	1.6	159	139/179	85	25/126	119	102/133
H4FC	1.6	117	100/139	151	75/226	142	97/156
H45CC	2	139	129/149	103	50/151	156	119/166
H8BC	4.3	0	-30/30	38	0/75	4	0/7
H8CC	4.3	50	20/80	50	25/75	7	3/11
H8FC	4.3	30	0/60	63	0/126	4	0/7
H9CC	4.8	30	0/60	75	25/151	7	0/11
H10CC	5.95	30	0/60	75	50/100	7	0/11
H11CC	8	10	-20/40	50	0/100	6	3/9
H12CC	10	0	-20/20	75	0/100	6	3/9
H13CC	11	0	-20/20	25	-25/75	6	4/9

[1] The NH_3 concentration was calculated from the subtraction factors given in Table 3, the peak absorbance for NH_3 at 965 cm^{-1}, and the correlation between absorbance and concentration shown in Figure 18B.

absorbance plot in Fig. 18b at 965 cm^{-1}. The resulting NH_3 concentrations are listed in Table 4, and the concentration *vs.* height in the combustion chamber is shown in Fig. 19.

CH_3CN Analysis. CH_3CN absorbs in several regions (cf. Fig 8 and 9). The absorption at 2200-2400 cm^{-1} and 600-750 cm^{-1} is, however, due to the presence of CO_2 in CH_3CN calibration gas (compare with H_2O reference which is also "contaminated" with small quantities of CO_2). With the present instrument, the band at 2590-2655 cm^{-1} appears to be most appropriate. At this wavenumber, interference from other species is insignificant. The absorption is weak and as a consequence the detection limit is rather high. The sample extracted from the bottom of the combustion chamber at a position 1.1 meter above the air nozzles did not contain a measurable quantity of CH_3CN, which means that its concentration is below 475 ppm (the lowest concentration of the available calibration spectra) if present. Since the coal nitrogen content is low and since only part of the fuel nitrogen will be present as CH_3CN, it seems likely that the concentration of CH_3CN should be considerably lower than 475 ppm. A gas cell with a longer optical path length would be required to measure CH_3CN at this frequency.

Conclusions

A gas sample extracted from a fluidised bed combustor contains a complex mixture of combustion reactants and products. Since most species interact with infrared light, FTIR analysis provides a versatile tool for qualitative as well as quantitative analysis. However, the high concentrations of CO_2, water vapour, CO and a large number of hydrocarbons complicate the analysis. In this

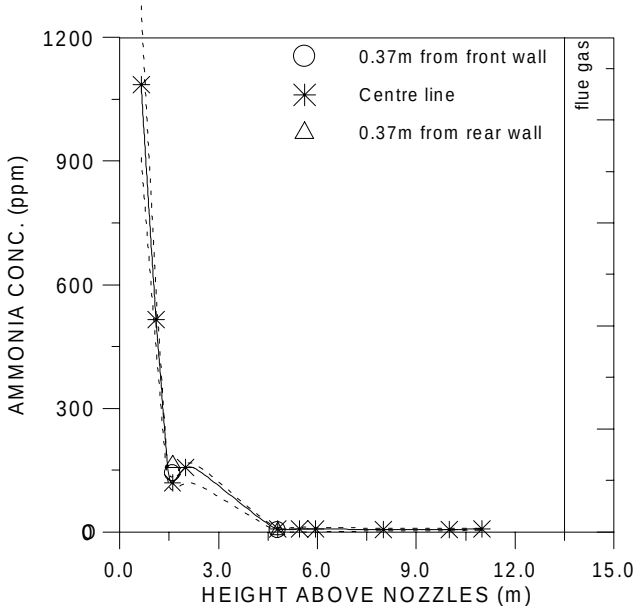

Fig. 19 Vertical profiles of NH_3 in the combustion chamber. Dotted lines indicate the uncertainty in the NH_3 determination.

report, the use of FTIR spectroscopy for HCN, HNCO, NH_3 and CH_3CN analysis is discussed.

NH_3 can be detected and quantified using the characteristic absorption peaks at 930 and 965 cm^{-1} where the major interfering components ethene and HNCO can be subtracted from the sample spectrum. HCN can be detected and quantified at 3200-3375 cm^{-1} where the major interfering component is H_2O. The low signal-to noise ratio makes the quantification rather uncertain. The major HCN peak at 714 cm^{-1} interferes with CO_2, and could not be used for quantification with the present instrument. This problem could possibly be resolved using an instrument with a higher resolution. Also the detection and quantification of HNCO should improve using an instrument with a higher resolution. The main peaks of absorption for HNCO interfere with the CO_2 absorption. Spectral subtraction of water, acetylene and CO_2 from the sample spectrum results in a spectrum where the presence of HNCO is indicated. The detection limit for CH_3CN is too high with the present instrument and CH_3CN could not be detected with the present instrument.

At a given cell path length, the total absorption of a sample can be reduced by diluting the sample with a non-absorbing gas. This method may enable quantification of trace components in regions where the absorption otherwise would be too high. A disadvantage is that the detection limits will increase and the dilution is not desired in all spectral regions and spectra from both diluted and non-diluted samples may be required.

Notation

$A(\nu)$ = absorbance
$a(\nu)$ = molar absorptivity (dm3 cm^{-1} moles $^{-1}$)
$B(\nu)$ = intensity of the source as a function of frequency ν
FWHH = full with at half-height

I(x) = intensity at the detector at a mirror displacement x of the movable mirror
SNR = signal-to-noise ratio
ν = frequency (Hz)
λ = wavelength (m)
σ = wave number (cm^{-1})
ρ = resolution parameter
$\tau(\nu)$ = transmittance
δ = retardation = optical path difference between movable and fixed mirror
Δ_{max} = maximum retardation of the interferometer

References

Brink, A., *Quantitative FT-IR analysis-Is it possible?,* Dept. Chemical Engineering, Report 92-121-A, 1992.

Griffiths, P.R., de Haseth, J.A., *Fourier Transform Infrared Spectroscopy,* Chemical Analysis, **83**, John Wiley & Sons, 1986.

Karlsson, M., Åmand, L.-E., *FTIR Analysis of Ammonia and Ethene in a Fluidized Bed Combustion Chamber,* Proceedings of the Third Nordic Conference on SOx and NOx from Heat and Power Generation, CHEC Report No.9610, Dept of Chemical Enginering, Techincal University of Denmark, Lyngby, pp. 93-97, 1996.

Karlsson, M., Åmand, L.-E., Leckner, B., *Comparison of FTIR and DOAS Measurement of NH_3 and NO in Fluidized Bed Combustion Gases.* Proceedings of the Finnish-Swedish Flame Days, IFRF, September 3-4, 1996, Naantali, Finland

Kassman, H., Åmand, L.-E., Leckner, B., *Secondary Effects in Sampling Ammonia during Measurements in a Circulating Fluidized-Bed Combustor, ,* Journal of the Institute of Energy, **70,** pp 95-101, 1997.

Kiss-Eröss, K., *Wilson and Wilson´s Comprehensive Analytical Chemistry,* Analytical Infrared Spectroscopy, **8**, (Ed. G: Svehla), Elsevier Scientific Publishing Company, 1976.

Rudling, L., *Undersökning av FTIR-teknik för rökgasanalys. Etapp 2,* Värmeforsk, Report No 444, Stiftelsen Värmeteknisk Forskning, In Swedish with an English summary, 1992.

Åmand, L.-E., Kassman, H., Karlsson, M., Leckner, B., *Measurement of the Concentration of Ammonia and Ethene in the Combustion Chamber of a Circulating Fluidized-Bed Boiler,* Journal of the Institute of Energy, **70,** pp 25-30, 1997.